Solitons in strongly driven discrete nonlinear Schrödinger-type models

Josselin Garnier,[1,*] Fatkhulla Kh. Abdullaev,[2] and Mario Salerno[3]
[1]*Laboratoire de Probabilités et Modèles Aléatoires and Laboratoire Jacques-Louis Lions, Université Paris VII, 2 Place Jussieu, 75251 Paris Cedex 5, France*
[2]*Physical-Technical Institute of the Uzbekistan Academy of Sciences, 700084, Tashkent-84, G. Mavlyanov street, 2-b, Uzbekistan*
[3]*Dipartimento di Fisica "E.R. Caianiello," Università di Salerno, 84081 Baronissi (SA), Italy*
(Received 30 October 2006; published 29 January 2007)

Discrete solitons in the Ablowitz-Ladik (AL) and discrete nonlinear Schrödinger (DNLS) equations with damping and strong rapid drive are investigated. The averaged equations have the forms of the parametric AL and DNLS equations. An additional type of parametric bright discrete soliton and cnoidal waves are found and the stability properties are analyzed. The analytical predictions of the perturbed inverse scattering transform are confirmed by the numerical simulations of the AL and DNLS equations with rapidly varying drive and damping.

DOI: 10.1103/PhysRevE.75.016615 PACS number(s): 05.45.Yv, 02.30.Jr, 03.75.Lm, 42.65.Tg

I. INTRODUCTION

Recently the problem of dynamics of nonlinear lattices under strong and rapid modulations of parameters has attracted a lot of attention. Two systems have been analyzed. The first one is the diffraction-managed array of optical waveguides, with diffraction varying periodically along the beam propagation [1]. The model is described by the discrete nonlinear Schrödinger (DNLS) equation with the coefficient of tunnel coupling between sites $c(t)$ rapidly and strongly varying in time:

$$iu_{nt} + \frac{1}{\epsilon} c\left(\frac{t}{\epsilon}\right)(u_{n+1} + u_{n-1}) + 2|u_n|^2 u_n = 0, \tag{1}$$

where $\epsilon \ll 1$. The analysis exhibits the existence of a type of discrete spatial optical solitons with beam width and peak amplitude evolving periodically during propagation.

The second system is the Bose-Einstein condensate in a periodic (in space) potential with a varying (in time) scattering length. In the tight-binding approximation this system is described by the DNLS equation [2] with a nonlinearity coefficient $\kappa(t)$ strongly and rapidly varying in time:

$$iu_{nt} + (u_{n+1} + u_{n-1}) + \frac{1}{\epsilon}\kappa\left(\frac{t}{\epsilon}\right)|u_n|^2 u_n = 0. \tag{2}$$

It was shown that this system supports nonlinearity-managed discrete solitons [3]. In a more general context it is of interest to investigate the influence of rapid perturbations on the dynamics of discrete solitons in nonlinear lattices. The case of strongly and rapidly varying external drivers is particularly important for applications. This problem is encountered both in the study of the dynamics of a magnetic flux quantum in an array of long Josephson junctions with varying ac current [4] and in the evolution of an optical field in a nonlinear chain of resonators or microcavities in the presence of pumping [5–8].

In this paper we consider the influence of a rapid strong drive on discrete bright solitons and cnoidal waves of the Ablowitz-Ladik (AL) and the DNLS equations with damping. Although the AL system has scarce physical applications it has many advantages from the analytical point of view, such as the complete integrability of the unperturbed system, existence of moving discrete solitons, etc. In some regions of the parameter space, the DNLS equation can be described as a perturbation of the AL model, a feature that we shall take advantage of in the following. The dynamics of discrete solitons in the AL and DNLS equations under the influence of damping and slowly varying driving field has been studied in Refs. [9,10]. Recently the influence of parametric drivers on the stability of strongly localized modes of the DNLS equation near the anticontinuum limit has been investigated in [11]. The stability of solitons in the continuous parametrically driven NLS equation has been studied in [12,13]. Here we address a general discrete nonlinear system with a strong rapid drive modeled by the following equation:

$$iu_{nt} + [u_{n+1} + u_{n-1} - (2+\omega)u_n] + |u_n|^2[(1-\chi)(u_{n+1} + u_{n-1}) + 2\chi u_n] = \frac{1}{\varepsilon} f\left(\frac{t}{\varepsilon}\right) - i\gamma u_n, \tag{3}$$

where f is a zero-mean periodic function with period 1 that describes the rapid drive, and the small parameter ε is the period of the drive. Here the parameter $\gamma \geq 0$ denotes the damping term, ω is the propagation constant in optics (chemical potential in Bose-Einstein condensates), and the parameter $\chi \in [0,1]$ characterizes the type of nonlinearity. For $\chi=0$ the nonlinearity is of intersite type as in the AL model while for $\chi=1$ we have the on-site nonlinearity of the DNLS equation. In absence of strong rapid drive and damping Eq. (3) coincides with the Salerno model [14] which interpolates between the AL model and the DNLS model. We show that, by averaging out the fast time scale, one can reduce Eq. (3), for particular choices of parameters, to the parametrically driven AL and DNLS equations with damping. The existence of parametric discrete bright solitons and

*Corresponding author. Electronic address: garnier@math.jussieu.fr

cnoidal waves of these equations is then investigated and the stability properties are studied both analytically and numerically. We find that the analytical predictions obtained from the averaged equations by means of a perturbation scheme based on the inverse scattering method are in good agreement with direct numerical simulations of the problem with rapidly varying drive and damping.

Finally, we remark that the physical systems where parametric discrete solitons of the type considered in this paper can be realized are chains of linearly coupled nonlinear microcavities [15] and nonlinear waveguide arrays with dielectric mirrors at the ends, driven by an external time-dependent field [7,8]. In this case the equation describing the discrete cavity solitons has the form of the parametric DNLS equation

$$iu_{nt} + \omega u_n + i\gamma u_n + \alpha|u_n|^2 u_n + C(u_{n+1} + u_{n-1} - 2u_n) = F_n(t), \tag{4}$$

where ω is the detuning from the linear resonance parameter, γ is the effective damping parameter, C is the effective coupling between adjacent waveguides, and $F_n(t)$ is the input field in the nth waveguide. Injecting a field that is homogeneous in space and rapidly varying in time, we can generate discrete parametric solitons in this system.

The paper is organized as follows. In Sec. II we derive the averaged DNLS-type equation for the strongly and rapidly varying external drive model. In Sec. III we analyze the solitons in a damped AL system with parametric drive. We use the perturbation theory based on the inverse scattering transform (IST) and study the stability region of parametric discrete solitons. Periodic solutions of the damped AL equation with parametric drive are also found in this section. The discrete soliton dynamics in the parametrically driven DNLS equation is investigated in Sec. IV.

II. AVERAGING

We look for the solution of Eq. (3) in the form

$$u_n(t) = u_n^{(0)}\left(t, \frac{t}{\varepsilon}\right) + \varepsilon u_n^{(1)}\left(t, \frac{t}{\varepsilon}\right) + \cdots, \tag{5}$$

where $u_n^{(0)}$, $u_n^{(1)}$, … are periodic in the argument $\tau = t/\varepsilon$. We substitute this ansatz into Eq. (3) and collect the terms with the same powers of ε. We obtain the hierarchy of equations

$$iu_{n\tau}^{(0)} = f(\tau),$$

$$iu_{nt}^{(0)} + [u_{n+1}^{(0)} + u_{n-1}^{(0)} - (2+\omega)u_n^{(0)}] + |u_n^{(0)}|^2[(1-\chi)(u_{n+1}^{(0)} + u_{n-1}^{(0)}) + 2\chi u_n^{(0)}] = -i\gamma u_n^{(0)} - iu_{n\tau}^{(1)}.$$

The first equation imposes the form of the leading-order term:

$$u_n^{(0)}(t,\tau) = -iF(\tau) + a_n(t),$$

where $F(\tau) = \int_0^\tau f(s)ds$ is the antiderivative of f and a_n depends only on the slow variable t. The second equation is the compatibility equation for the existence of the expansion (5). By integrating over a period in τ, we obtain

$$ia_{nt} + [a_{n+1} + a_{n-1} - (2+\omega)a_n] + (1-\chi)\langle|a_n - iF(\cdot)|^2[a_{n+1} + a_{n-1} - 2iF(\cdot)]\rangle + 2\chi\langle|a_n - iF(\cdot)|^2[a_n - iF(\cdot)]\rangle = -i\gamma a_n$$

which gives

$$ia_{nt} + [a_{n+1} + a_{n-1} - (2+\omega)a_n] + |a_n|^2[(1-\chi)(a_{n+1} + a_{n-1}) + 2\chi a_n] = -i\gamma a_n + \delta\overline{a_n} - \frac{\delta}{2}[(1-\chi)(a_{n+1} + a_{n-1}) + 2(1+\chi)a_n], \tag{6}$$

where $\delta = 2\langle F^2\rangle$.

Thus, the averaging method applied to Eq. (3) leads to a *parametrically driven* nonlinear lattice equation which reduces to the Salerno model [14] in the absence of perturbations. It is possible to consider a random forcing instead of a periodic one. More precisely, we get the same result if the source $f(\tau)$ is a colored noise with coherence time of order 1. However, the power spectral density of the source should vanish at zero frequency. Otherwise it would appear as a phase diffusion and this would destroy the stability of the stationary solution that we will introduce next.

We introduce the rescaled time $T = t[1 + \delta(1-\chi)/2]$ and the rescaled function $A_n = a_n/\sqrt{1 + \delta(1-\chi)/2}$. The averaged equation for the function $A_n(T)$ has the form

$$iA_{nT} + [A_{n+1} + A_{n-1} - (2+\Omega)A_n] + |A_n|^2(A_{n+1} + A_{n-1}) = R_n, \tag{7}$$

$$R_n = -i\Gamma A_n + \Delta\overline{A_n} + \chi|A_n|^2(A_{n+1} + A_{n-1} - 2A_n), \tag{8}$$

where

$$\Delta = \frac{\delta}{1 + \delta(1-\chi)/2}, \quad \Gamma = \frac{\gamma}{1 + \delta(1-\chi)/2},$$

$$\Omega = \frac{\omega - 2\delta}{1 + \delta(1-\chi)/2}.$$

The left-hand side of (7) is the Ablowitz-Ladik equation, which is completely integrable. The right-hand side can be seen as a perturbation of this system. We shall use the perturbed inverse scattering transform to study the evolution dynamics of AL solitons driven by the perturbation R_n.

III. THE DAMPED AL SYSTEM WITH PARAMETRIC DRIVE

We consider in this section the case $\chi=0$, that is, the AL model with damping and rapid drive. Therefore, we consider the perturbed AL equation (7) with the perturbation

$$R_n = -i\Gamma A_n + \Delta\overline{A_n}. \tag{9}$$

A. Perturbed inverse scattering transform

We assume that the damping parameter γ and the parametric drive parameter δ are small (but ω can be of order 1). Therefore, Γ and Δ are small, and, following [16–18], the evolution equations for the soliton parameters in the adiabatic approximation have the form

$$x_T = 2\frac{\sinh\beta}{\beta}\sin\alpha + \frac{\sinh\beta}{\beta}\sum_{n=-\infty}^{\infty}\frac{(n-x)\cosh\beta(n-x)\mathrm{Im}(r_n)}{\cosh\beta(n+1-x)\cosh\beta(n-1-x)},$$

$$\beta_T = \sinh\beta\sum_{n=-\infty}^{\infty}\frac{\cosh\beta(n-x)\mathrm{Im}(r_n)}{\cosh\beta(n+1-x)\cosh\beta(n-1-x)},$$

$$\alpha_T = \sinh\beta\sum_{n=-\infty}^{\infty}\frac{\sinh\beta(n-x)\mathrm{Re}(r_n)}{\cosh\beta(n+1-x)\cosh\beta(n-1-x)},$$

$$\sigma_T = 2\cosh\beta\cos\alpha + 2\frac{\sinh\beta}{\beta}\alpha\sin\alpha - 2 - \Omega + \sinh\beta\sum_{n=-\infty}^{\infty}\frac{(n-x)\sinh\beta(n-x)\mathrm{Re}(r_n)}{\cosh\beta(n+1-x)\cosh\beta(n-1-x)} - \cosh\beta\sum_{n=-\infty}^{\infty}\frac{\cosh\beta(n-x)\mathrm{Re}(r_n)}{\cosh\beta(n+1-x)\cosh\beta(n-1-x)} + \alpha\frac{\sinh\beta}{\beta}\sum_{n=-\infty}^{\infty}\frac{(n-x)\cosh\beta(n-x)\mathrm{Im}(r_n)}{\cosh\beta(n+1-x)\cosh\beta(n-1-x)},$$

where $r_n = R_n\exp[-i\alpha(n-x)-i\sigma]$. Using standard analytical tools (Poisson summation formula and residue theorem), we can compute the right-hand sides of these equations. The equation for β takes the form

$$\beta_T = \Delta P^{(\beta)} + \Gamma G^{(\beta)}, \tag{10}$$

where

$$P^{(\beta)} = -\sinh^2\beta\sum_{s=-\infty}^{\infty} I_\beta(2\alpha + 2\pi s)\sin(2\pi s x + 2\sigma),$$

$$G^{(\beta)} = -2\tanh\beta,$$

with

$$I_\beta(a) = \frac{2\pi\sin a}{\beta\sinh(2\beta)\sinh[\pi a/(2\beta)]}.$$

The equation for α has the form

$$\alpha_T = \Delta P^{(\alpha)} + \Gamma G^{(\alpha)}, \tag{11}$$

where

$$P^{(\alpha)} = -\sinh^2\beta\sum_{s=-\infty}^{\infty} K_\beta(2\alpha + 2\pi s)\sin(2\pi s x + 2\sigma),$$

$$G^{(\alpha)} = 0,$$

with

$$K_\beta(a) = \frac{2\pi\sin^2(a/2)}{\beta\sinh^2\beta\sinh[\pi a/(2\beta)]}.$$

The equation for the soliton center x has the form

$$x_T = 2\frac{\sinh\beta}{\beta}\sin\alpha + \Delta P^{(x)} + \Gamma G^{(x)}, \tag{12}$$

where

$$P^{(x)} = -\frac{\sinh^2\beta}{\beta}\sum_{s=-\infty}^{\infty} J_\beta(2\alpha + 2\pi s)\cos(2\pi s x + 2\sigma),$$

$$G^{(x)} = -\frac{\sinh^2\beta}{\beta}\psi_\beta(x),$$

with $J_\beta(a) = -I'_\beta(a)$ and

$$\psi_\beta(x) = \sum_{n=-\infty}^{\infty}\frac{(n-x)}{\cosh\beta(n+1-x)\cosh\beta(n-1-x)} = \frac{4\pi}{\beta\sinh(2\beta)}\sum_{s=1}^{\infty}\frac{\sin(2\pi s x)}{\sinh(\pi^2 s/\beta)}.$$

Finally, the equation for the soliton phase σ has the form

$$\sigma_T = 2\cosh\beta\cos\alpha + 2\frac{\sinh\beta}{\beta}\alpha\sin\alpha - 2 - \Omega + \Delta P^{(\sigma)} + \Gamma G^{(\sigma)}, \tag{13}$$

where

$$P^{(\sigma)} = -\sinh\beta \sum_{s=-\infty}^{\infty} L_\beta(2\alpha + 2\pi s)\cos(\alpha + \pi s + 2\sigma + 2\pi s x)$$

$$+ \sinh\beta \sum_{s=-\infty}^{\infty} K'_\beta(2\alpha + 2\pi s)\sin(2\pi s x + 2\sigma)$$

$$- \sinh\beta \sum_{s=-\infty}^{\infty} K_\beta(2\alpha + 2\pi s)\cos(2\pi s x + 2\sigma)$$

$$- \frac{\alpha \sinh^2\beta}{2\beta} \sum_{s=-\infty}^{\infty} I'_\beta(2\alpha + 2\pi s)\sin(2\pi s x + 2\sigma),$$

$$G^{(\sigma)} = -\alpha \frac{\sinh^2\beta}{\beta}\psi_\beta(x),$$

with

$$L_\beta(a) = \frac{2\pi \sin(a/2)}{\beta \sinh\beta \sinh[\pi a/(2\beta)]}.$$

B. Parametrically driven AL solitons

The system (10)–(13) has zero fixed points if $\Gamma > \Delta$ (which is equivalent to $\gamma > \delta$), or $\Gamma \le \Delta$ but $\Omega < -\sqrt{\Delta^2 - \Gamma^2} < 0$ (which is equivalent to $\gamma \ge \delta$ and $\omega < 2\delta - \sqrt{\delta^2 - \gamma^2}$); one fixed point if $\Gamma \le \Delta$ and $-\sqrt{\Delta^2 - \Gamma^2} \le \Omega < \sqrt{\Delta^2 - \Gamma^2}$ (which is equivalent to $2\delta - \sqrt{\delta^2 - \gamma^2} \le \omega < 2\delta + \sqrt{\delta^2 - \gamma^2}$) [this fixed point is the one labeled + in Eqs. (14) and (15)]; two fixed points if $\Gamma \le \Delta$and $\Omega \ge \sqrt{\Delta^2 - \Gamma^2}$ (which is equivalent to $\omega \ge 2\delta + \sqrt{\delta^2 - \gamma^2}$):

$$\alpha_\pm = 0, \quad \sin(2\sigma_\pm) = -\frac{\Gamma}{\Delta}, \quad \cos(2\sigma_\pm) = \pm\sqrt{1 - \frac{\Gamma^2}{\Delta^2}}, \tag{14}$$

$$\beta_\pm = \operatorname{arccosh}\left(1 + \frac{\Omega}{2} \pm \frac{1}{2}\sqrt{\Delta^2 - \Gamma^2}\right). \tag{15}$$

The center of the soliton can be arbitrary. It is remarkable that these values correspond not only to fixed points of the system (10)–(13), but also to fixed points of the averaged partial differential equation (7). Indeed, the two solitons labeled ±,

$$A_n(T) = \frac{\sinh\beta_\pm}{\cosh[\beta_\pm(n - x_\pm)]} e^{i\sigma_\pm},$$

are exact solutions of Eq. (7) with $\chi = 0$.

We can investigate the linear stability of these solutions. The linearization of the nonlinear system (10)–(13) around the parameters of the stationary solitons gives the linear system

$$\beta_{1T} = -2\Delta \sinh^2\beta_\pm \psi_{\beta_\pm}(x_\pm)\cos(2\sigma_\pm)\alpha_1$$

$$- 4\Delta \tanh\beta_\pm \cos(2\sigma_\pm)\sigma_1, \tag{16}$$

$$\alpha_{1T} = -2\Gamma\alpha_1, \tag{17}$$

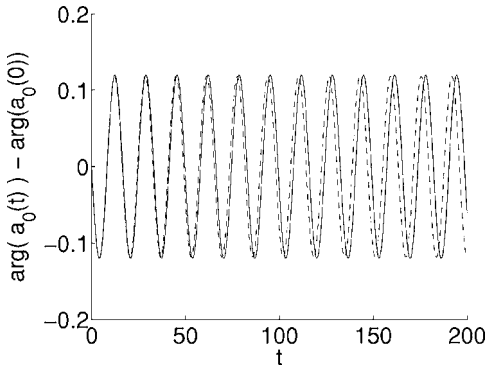

FIG. 1. Here $\chi = 0$, $\omega = 1$, $\delta = 0.022$, and $\gamma = 0$ (i.e., $\Delta = 0.0218$ and $\Gamma = 0$). The initial condition is a soliton with $\sigma = \sigma_+$, $x_+ = 0$, $\alpha = 0$, and $\beta = \beta_+ + 0.02$ ($\beta_+ = 0.948$). We plot the solution phase obtained from the numerical integration of Eq. (6) (dashed line) and compare with the theoretical oscillation obtained from (16)–(18) (solid line). The theoretical oscillation period (in the t variable) is $2\pi/\Omega_+/(1 + \delta/2) = 16.6$.

$$\sigma_{1T} = 2\sinh\beta_\pm\beta_1 - 2\Gamma\sigma_1, \tag{18}$$

$$x_{1T} = 2\frac{\sinh\beta_\pm}{\beta_\pm}\alpha_1 - \Delta\frac{\sinh^2\beta_\pm}{\beta_\pm}\frac{\pi^2 + 4\beta_\pm^2}{3\beta_\pm^2\sinh(2\beta_\pm)}\cos(2\sigma_\pm)\alpha_1$$

$$- \Gamma\frac{\sinh^2\beta_\pm}{\beta_\pm}\psi'_{\beta_\pm}(x_\pm)x_1$$

$$- \Gamma\frac{\beta_\pm\sinh(2\beta_\pm) - \sinh^2\beta_\pm}{\beta_\pm^2}\psi_{\beta_\pm}(x_\pm)\beta_1. \tag{19}$$

The equation for x_1 is decoupled from the other ones. The three eigenvalues for the 3×3 system for $(\alpha_1, \beta_1, \sigma_1)$ are

$$\lambda_\pm^{(1)} = -2\Gamma,$$

$$\lambda_\pm^{(2)} = -\Gamma + \sqrt{\Gamma^2 - 8\Delta\sinh\beta_\pm\tanh\beta_\pm\cos(2\sigma_\pm)},$$

$$\lambda_\pm^{(3)} = -\Gamma - \sqrt{\Gamma^2 - 8\Delta\sinh\beta_\pm\tanh\beta_\pm\cos(2\sigma_\pm)}.$$

The fixed point is stable if the real parts of the eigenvalues are nonpositive. This shows that the fixed point labeled − is unstable, since $\lambda_-^{(2)} > 0$, while the fixed point labeled + is stable.

In the absence of damping $\Gamma = 0$ (which is equivalent to $\gamma = 0$), the soliton parameters β and σ (amplitude and phase) oscillate with the frequency (in the T variable)

$$\Omega_+ = \sqrt{8\Delta\sinh\beta_+\tanh\beta_+} \tag{20}$$

while the parameter α (velocity) is constant. This means that the stationary soliton is stable. This also shows that stable slowly moving breathers can propagate in the presence of parametric drive.

We have performed numerical simulations of Eq. (6) to confirm these predictions. In Fig. 1 we consider a perturbation of the initial amplitude. The periodic oscillations of the soliton parameters have the predicted period (20). In Fig. 2 we consider a soliton with a positive velocity. As predicted by the theory, this soliton can propagate in a stable way.

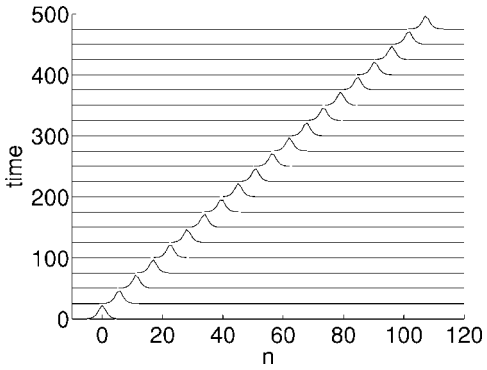

FIG. 2. Here $\chi=0$, $\omega=1$, $\delta=0.022$, $\gamma=0$. The initial condition is a soliton with $\sigma=\sigma_+$, $x_+=0$, $\alpha=0.1$, and $\beta=\beta_+$. We plot the soliton profiles $|a_n(t)|$ at different times, which exhibits the stable propagation of the moving soliton.

In the presence of damping the soliton parameters β and σ oscillate with the frequency

$$\Omega_+ = \sqrt{8\sqrt{\Delta^2 - \Gamma^2}\sinh\beta_+ \tanh\beta_+ - \Gamma^2}. \tag{21}$$

These oscillations decay exponentially with the rate Γ. In addition, comparing (20) and (21) shows that the damping enhances the oscillation period. In Fig. 3, right upper, we plot the damping of the oscillations of the soliton parameters obtained from the averaged equation (6) and compare it to the theoretical formula. We have also simulated the original

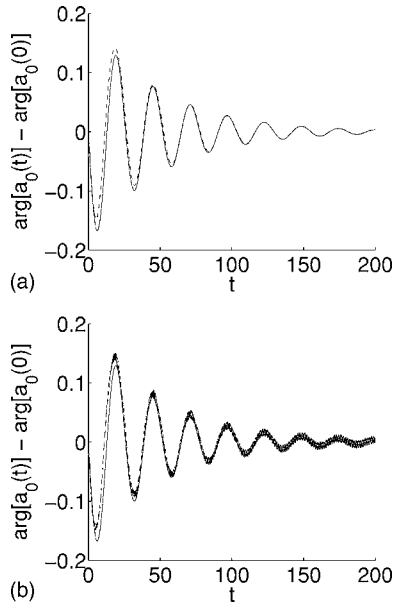

FIG. 3. Here $\chi=0$, $\omega=1$, $\delta=0.022$, $\gamma=0.02$. The initial condition is a soliton with $\sigma=\sigma_+$, $x_+=0$, $\alpha=0$, and $\beta=\beta_+ + 0.02$ ($\beta_+ = 0.942$). We integrate numerically the averaged equation (6) and plot the phase of $a_0(t)$ (dashed line) in the upper panel. We integrate numerically the original equation (3) and plot the phase of $a_0(t) := u_0(t) + i\sin(16\pi t)$ (dashed line) in the lower panel. The oscillations and damping given by the original equation and by the averaged equation are the same, and they are correctly predicted by the model (16)–(18) (solid line). The period is $2\pi/\Omega_+/(1+\delta/2)=25.9$ and the exponential decay rate is $\gamma=0.02$.

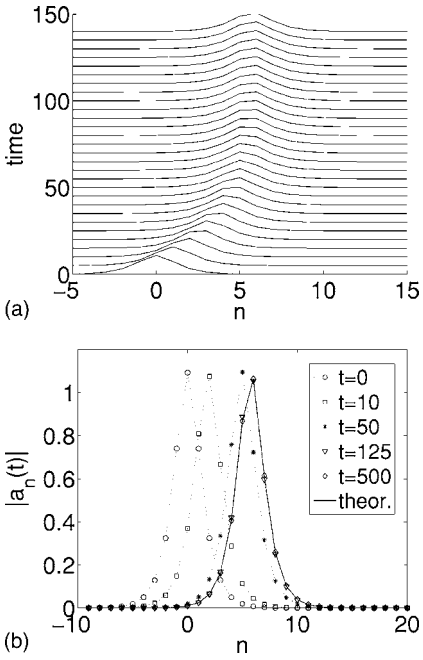

FIG. 4. Here $\chi=0$, $\omega=1$, $\delta=0.022$, $\gamma=0.02$. The initial condition is a soliton with $\sigma=\sigma_+$, $x_+=0$, $\alpha=0.1$, and $\beta=\beta_+$. We plot the soliton profiles $|a_n(t)|$ at different times, which exhibits the trapping of the moving soliton. In the lower panel, the solid line is the theoretical stationary soliton centered at $x_F=5.76$ given by (23).

equation (3) with the external drive $f(\tau)=\sin(2\pi\tau)$ and $\varepsilon=0.125$. We plot one of the obtained results in Fig. 3, lower panel, which shows full agreement.

The system of equations (16)–(19) predicts that the soliton parameter α decays exponentially at the rate 2Γ. Since this parameter determines the velocity, this shows that the propagation of moving solitons is not supported. If we denote by α_0 the initial value of the parameter α, then the soliton approaches the asymptotic form

$$A_n = \frac{\sinh\beta_+}{\cosh[\beta_+(n - x_+ - x_F)]} e^{i\sigma_+} \tag{22}$$

with a rate of order $\exp(-2\Gamma t)$, where the asymptotic position is given by

$$x_F = \frac{\sinh\beta_+ \sin\alpha_0}{\beta_+\Gamma}. \tag{23}$$

In Fig. 4 the trapping of a soliton with an initial positive velocity is shown. The asymptotic position x_F of the soliton as predicted by the perturbed IST is given by (23). We plot the theoretical soliton shape centered at x_F and compare it with the solution obtained from numerical simulations. After time $t=100$ the soliton no longer moves and its position and shape coincide exactly with (22) and (23), respectively.

C. Periodic solutions of the damped AL equation with parametric drive

In the following we discuss exact periodic solutions of the parametrically damped and driven AL equation

$$iA_{nT} + [A_{n+1} - (2+\Omega)A_n + A_{n-1}] + [i\eta + (1+i\eta)|A_n|^2](A_{n+1} + A_{n-1}) = -i\Gamma A_n + \Delta\overline{A_n}, \tag{24}$$

where $\eta \geq 0$ models a small dispersive and nonlinear damping. In this regard we consider periodic stationary solutions of the form

$$A_n = Ae^{i\sigma}\mathrm{dn}[\beta(n+x_F),m]. \tag{25}$$

Direct substitution of Eq. (25) into Eq. (24) shows that a solution is indeed obtained provided the two following relations are satisfied by the soliton parameter β and the modulus m:

$$2+\Omega-2\frac{\mathrm{dn}(\beta,m)}{\mathrm{cn}(\beta,\mathrm{m})^2}+\Delta\left[1-\left(\frac{\Gamma}{\Delta}+\frac{2\eta\mathrm{dn}(\beta,m)}{\Delta\mathrm{cn}(\beta,m)^2}\right)^2\right]^{1/2}=0, \tag{26}$$

$$\beta N_p = 2K(m), \tag{27}$$

where N_p is the number of sites in one period and $K(m)$ is the complete elliptic integral of the first kind. Here $m \in (0,1)$ and N_p must be a positive integer, so that there exists a numerable set of pairs (β,m) that satisfy the conditions (26) and (27). If the conditions are satisfied, then the periodic function (25) is a solution of (24) with the amplitude A and phase σ given by

$$A = \pm\frac{\mathrm{sn}(\beta,m)}{\mathrm{cn}(\beta,m)}, \quad \sigma = -\frac{1}{2}\arcsin\left(\frac{\Gamma}{\Delta}+\frac{2\eta\mathrm{dn}(\beta,m)}{\Delta\mathrm{cn}(\beta,m)^2}\right), \tag{28}$$

while the soliton center x_F is arbitrary.

Another periodic solution of Eq. (24) can be constructed by replacing the function dn into the ansatz (25) with the elliptic cosine cn:

$$A_n = Ae^{i\sigma}\mathrm{cn}[\beta(n+x_F),m]. \tag{29}$$

In this case the two conditions to be satisfied by β and m are

$$2+\Omega-2\frac{\mathrm{cn}(\beta,m)}{\mathrm{dn}(\beta,m)^2}+\Delta\left[1-\left(\frac{\Gamma}{\Delta}+\frac{2\eta\mathrm{cn}(\beta,m)}{\Delta\mathrm{dn}(\beta,m)^2}\right)^2\right]^{1/2}=0, \tag{30}$$

$$\beta N_p = 4K(m), \tag{31}$$

and the soliton amplitude and phase are

$$A = \pm\sqrt{m}\frac{\mathrm{sn}(\beta,m)}{\mathrm{dn}(\beta,m)}, \quad \sigma = -\frac{1}{2}\arcsin\left(\frac{\Gamma}{\Delta}+\frac{2\eta\mathrm{cn}(\beta,m)}{\Delta\mathrm{dn}(\beta,m)^2}\right). \tag{32}$$

It may be worth noting that in deriving these solutions usage of the following identities for the Jacobi elliptic functions [19] has been made:

$$\mathrm{dn}(x+a,m)+\mathrm{dn}(x-a,m)=\frac{2\mathrm{dn}(a,m)\mathrm{dn}(x,m)}{\mathrm{cn}(a,m)^2+\mathrm{sn}(a,m)^2\mathrm{dn}(x,m)^2}, \tag{33}$$

$$\mathrm{cn}(x+a,m)+\mathrm{cn}(x-a,m)=\frac{2\mathrm{cn}(a,m)\mathrm{cn}(x,m)}{\mathrm{dn}(a,m)^2+m\mathrm{sn}(a,m)^2\mathrm{cn}(x,m)^2}. \tag{34}$$

Also notice that in the limit of infinite period (i.e., $m \to 1$) the above solutions both reduce to trains of well-separated AL solitons of the form

$$A_n = \frac{\sinh(\beta)}{\cosh[\beta(n+x_F)]}e^{i\sigma}, \tag{35}$$

with the soliton parameter satisfying

$$2+\Omega+\{\Delta^2-[\Gamma+2\eta\cosh(\beta)]^2\}^{1/2}-2\cosh(\beta)=0.$$

For $\eta=0$ these equations reproduce the result in Eqs. (14) and (15) of the previous section. Similar periodic solutions exist also for the unperturbed AL equation [20] and for generalized AL equations with arbitrarily high-order nonlinearities [21].

In Fig. 5 we depict the waveforms of the above solutions

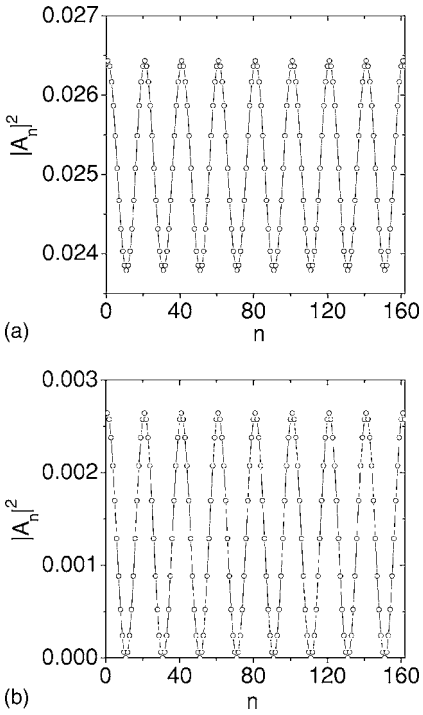

FIG. 5. Upper panel: Square modulus of the dn solution in Eq. (25) with $m=0.1$, $\beta=0.161\,244$ ($N_p=20$), $x_F=0$, on a line of 160 points. The parameters are fixed as $\Delta=0.04$, $\Gamma=0.02$, $\Omega=0.015\,58$, $\eta=0$. Lower panel: Square modulus of the cn solution in Eq. (29) with parameters fixed as in the upper panel.

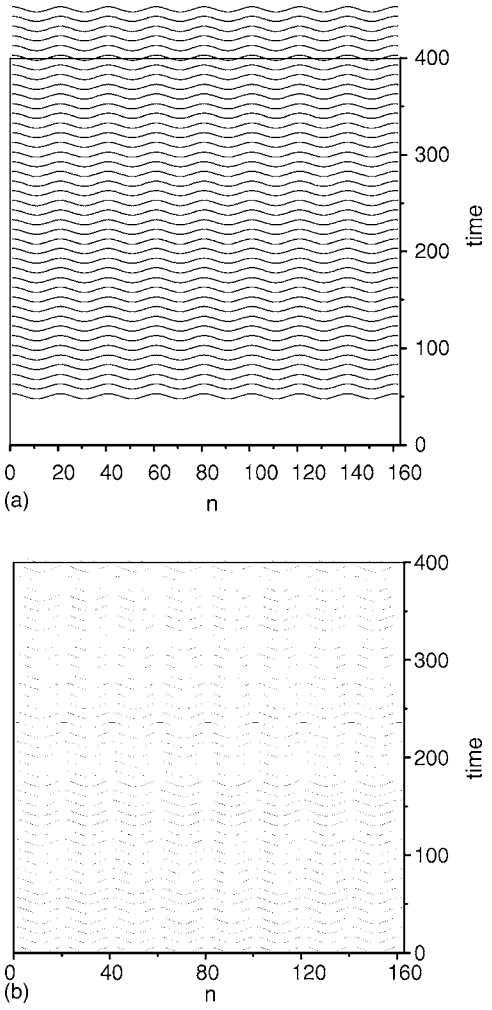

FIG. 6. Time evolution of $|A_n|^2$ for the dn (upper panel) and cn (lower panel) solutions in Fig. 5.

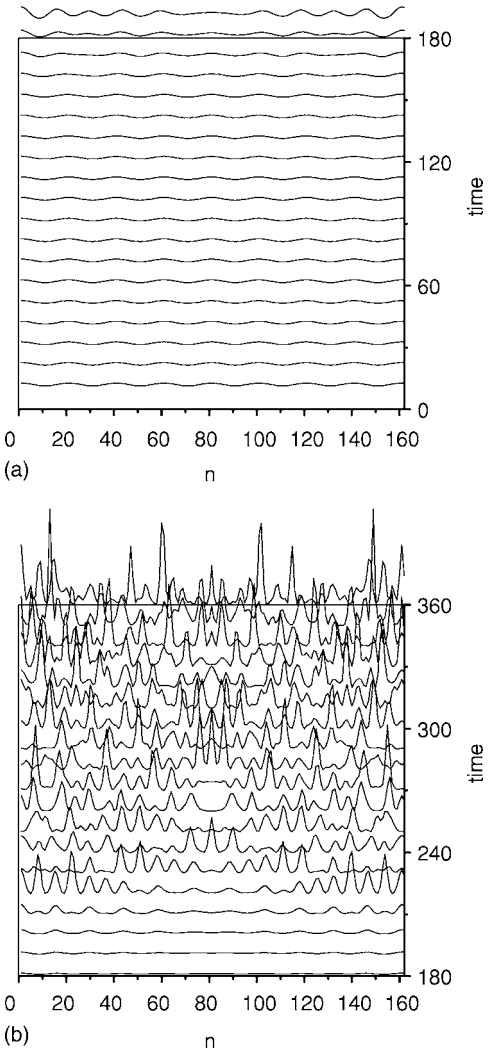

FIG. 7. Time evolution of the unstable dn solution in Eq. (25) obtained for $\Delta=0.15$, $\Gamma=0.02$, $\Omega=-0.098\,438$, $\eta=0$, and the solution parameters as in Fig. 5: $m=0.1$, $\beta=2K(m)/N_p=0.161\,244$, $N_p=20$. Notice the change in the $|A_n|^2$ scale from one panel to another.

on a line of 160 points for the case $\Delta=0.04$, $\Gamma=0.02$, $\Omega=0.015\,58$, $\eta=0$, and the solution parameters are $m=0.1$, $\beta=2K(m)/N_p=0.161\,244$, $N_p=20$. We find, by direct numerical integrations of Eq. (24), that for small values of the damping and parametric driver amplitude these solutions remain stable under very long time evolution. This is shown in Fig. 6 where the time evolution obtained from direct numerical simulations of Eq. (24) is depicted for parameters $\Delta=0.15$, $\Gamma=0.02$, $\Omega=-0.098\,438$, $\eta=0$, which supports the same dn and cn solutions as in Fig. 5. By keeping fixed the damping constant and increasing the amplitude of the parametric driver in a certain range, we find that these solutions remain stable for a very long time, while outside of this range instabilities quickly develop. The development of the instability for out-of-range parameters is investigated in Figs. 7 and 8.

Notice that while for the dn solution the instability suddenly sets in without any apparent pattern, the instability of the cn solution seems to follow a precise pattern. In particular, from Fig. 8, we see that before the instability fully develops—at time $t\approx 200$—the cn solution bifurcates into a period three solution at $t\approx 80$, which remains stable for a long time. The presence of a small dispersive nonlinear damping (controlled by the parameter η) effectively increases the stability of both the period one and the period three solutions, as one can see from Fig. 9. The scenario behind the development of the instability of the cn solution is quite interesting and deserves more investigation.

IV. THE DAMPED DNLS SYSTEM WITH PARAMETRIC DRIVE

We consider in this section that the nonlinear term is not of the AL type but is a mixture of the AL cubic intersite nonlinearity and the on-site DNLS cubic term. We shall analyze this system by considering such a nonlinearity as a perturbation of the cubic AL nonlinearity.

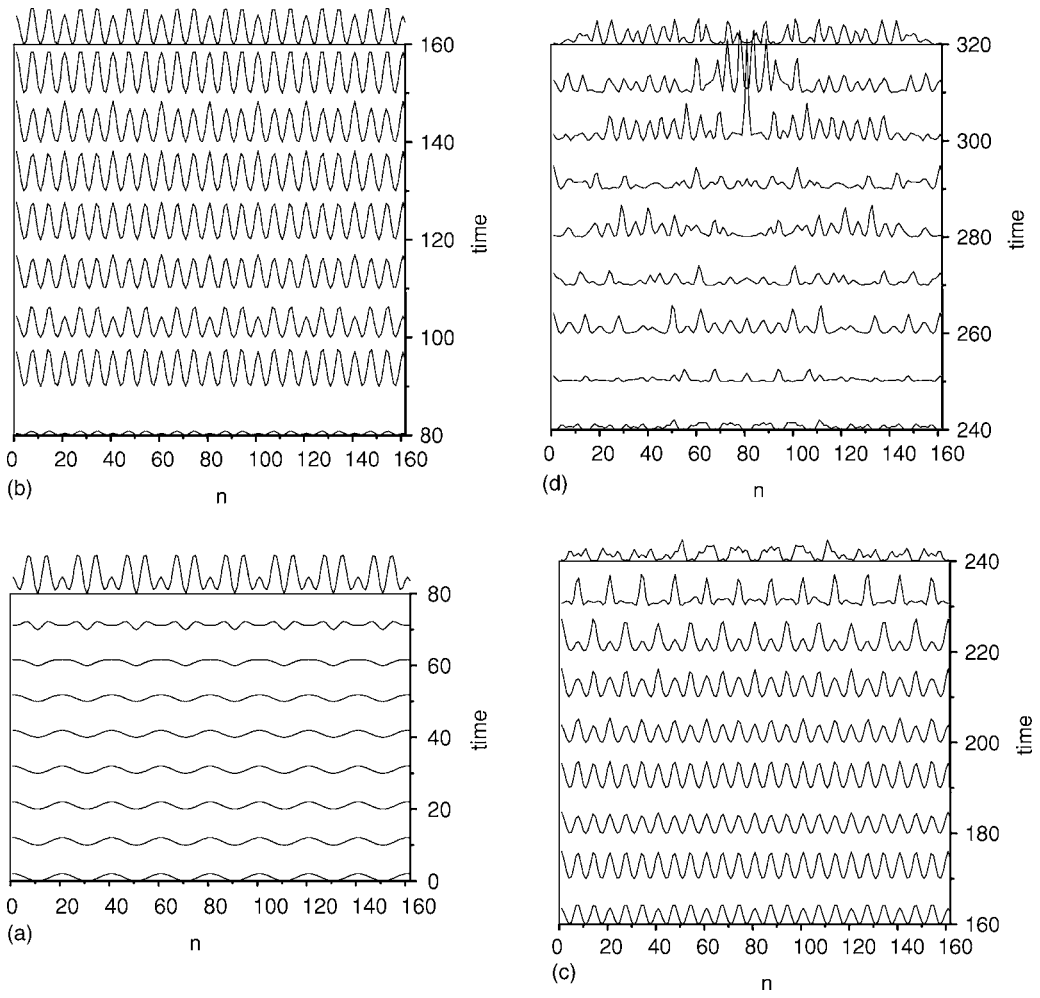

FIG. 8. Time evolution of the unstable cn solution in Eq. (29) when the parameters are fixed as in Fig. 5. Notice the change in the $|A_n|^2$ scale passing from one panel to another.

A. Perturbation theory for the cubic nonlinearity

In this section we consider the perturbed AL equation (7) when the perturbation is given by

$$R_n = \chi |A_n|^2 (A_{n+1} + A_{n-1} - 2A_n). \tag{36}$$

If $\chi=0$, then Eq. (7) with the perturbation (36) is the integrable AL equation. If $\chi=1$, then it is the standard DNLS equation. In the adiabatic approximation, this perturbation has no effect on the first-order differential equation for the amplitude soliton parameter β, but the evolution equations for the parameters x, α, and σ have corrective terms

$$x_T = 2(1-\chi)\frac{\sinh\beta}{\beta}\sin\alpha + 2\chi\frac{\sinh^2\beta}{\beta^2\cosh\beta}\sin\alpha, \tag{37}$$

$$\alpha_T = \chi P_\beta(x), \tag{38}$$

$$\sigma_T = 2\cosh\beta\cos\alpha + 2\chi(1-\cos\alpha)\sinh\beta\tanh\beta + 2(1-\chi)\alpha\sin\alpha\frac{\sinh\beta}{\beta} + 2\chi\alpha\sin\alpha\frac{\sinh^2\beta}{\beta^2\cosh\beta} - 2 - \Omega + 2\chi Q_\beta(x), \tag{39}$$

where

$$P_\beta(x) = \sum_{s=1}^{\infty} \frac{8\pi^3 s^2 \sinh^2\beta}{\beta^3 \sinh(\pi^2 s/\beta)} \sin(2\pi s x), \tag{40}$$

$$Q_\beta(x) = -1 + \frac{\sinh 2\beta}{\beta} - \frac{\sinh^2\beta}{\beta^2} - \sinh\beta\tanh\beta + 2\sum_{s=1}^{\infty} \frac{2\pi^2 s\beta^2 \sinh\beta\cosh\beta + [\pi^4 s^2 \mathrm{cotanh}(\pi^2 s/\beta) - 2\pi^2 s\beta]\sinh^2\beta}{\beta^4 \sinh(\pi^2 s/\beta)} \cos(2\pi s x). \tag{41}$$

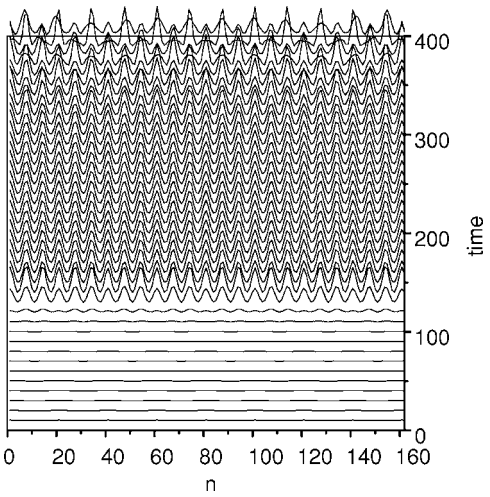

FIG. 9. Time evolution of the unstable dn solution in Eq. (25) obtained for $\eta=0.02$. Other parameters are fixed as in Fig. 8.

We should keep in mind that the adiabatic approximation is valid when the perturbation (36) is small, which is true if χ is small and β is arbitrary, or if χ is arbitrary and β is small. In the following, we shall keep only the term $s=1$ in the sums [Eqs. (40) and (41)], to simplify the algebra, although the analysis could be carried out with the full expressions. This simplification is consistent with the adiabatic approximation.

B. Parametrically driven DNLS solitons

We now consider that the perturbation R_n is given by Eq. (8), that is, the sum of the cubic perturbation Eq. (36) and the parametric drive with damping Eq. (9). In these conditions, there are two fixed points if $\Gamma<\Delta$ (which is equivalent to $\gamma<\delta$) and $\Omega+\Delta>0$ (which is equivalent to $\omega-\delta>0$):

$$\alpha_\pm = 0, \quad \sin(2\sigma_\pm) = -\frac{\Gamma}{\Delta}, \quad \cos(2\sigma_\pm) = \pm\sqrt{[1-(\Gamma^2/\Delta^2)]}, \tag{42}$$

$$\cosh(\beta_\pm) - 1 + \chi Q_{\beta_\pm}(0) = \frac{\Omega}{2} + \frac{1}{2}\sqrt{\Delta^2-\Gamma^2}. \tag{43}$$

The center of the soliton $x_\pm$ must be an integer as soon as $\chi>0$. This is a manifestation of the Peierls-Nabarro barrier [16,22]. Note that the function $\beta\mapsto\cosh(\beta)-1+\chi Q_\beta(0)$ is a one-to-one increasing function from $(0,\infty)$ to $(0,\infty)$ for any $\chi\geq 0$. Therefore, the parameter $\beta_\pm$ is uniquely determined. The picture is the same as in the perturbed AL case. The only difference is a renormalization of the amplitude parameter $\beta_\pm$ given by Eq. (43) instead of Eq. (15).

We next perform the linear stability analysis of the fixed points. The linearization of the system of ordinary differential equations for the soliton parameters around the stationary points gives:

$$\beta_{1T} = -4\Delta\tanh\beta_\pm\cos(2\sigma_\pm)\sigma_1, \tag{44}$$

$$\alpha_{1T} = -2\Gamma\alpha_1 + 16\pi^4\chi\frac{\sinh^2\beta_\pm}{\beta_\pm^3\sinh\left(\frac{\pi^2}{\beta_\pm}\right)}x_1, \tag{45}$$

$$\sigma_{1T} = 2[\sinh\beta + \chi\partial_\beta Q_\beta(0)]_{\beta=\beta_\pm}\beta_1 - 2\Gamma\sigma_1, \tag{46}$$

$$\begin{aligned} x_{1T} = {} & 2(1-\chi)\frac{\sinh\beta_\pm}{\beta_\pm}\alpha_1 + 2\chi\frac{\sinh^2\beta_\pm}{\beta_\pm^2\cosh\beta_\pm}\alpha_1 \\ & - \Delta\frac{\tanh\beta_\pm}{\beta_\pm^3}\frac{\pi^2+4\beta_\pm^2}{6}\cos(2\sigma_\pm)\alpha_1 \\ & - \Gamma\frac{\tanh\beta_\pm}{\beta_\pm^2}\frac{4\pi^2}{\sinh\left(\frac{\pi^2}{\beta_\pm}\right)}x_1. \end{aligned} \tag{47}$$

This 4×4 linear system can be decomposed into two 2×2 linear systems, for (β_1,σ_1) and for (α_1,x_1), respectively. It is then easy to compute the eigenvalues. They are:

$$\lambda_\pm^{(1)} = -\Gamma + \Omega_\pm,$$

$$\lambda_\pm^{(2)} = -\Gamma - \Omega_\pm,$$

$$\lambda_\pm^{(3)} = -\Gamma\left[1 + \frac{\tanh\beta_\pm}{\beta_\pm^2}\frac{2\pi^2}{\sinh\left(\frac{\pi^2}{\beta_\pm}\right)}\right] + \tilde{\Omega}_\pm,$$

$$\lambda_\pm^{(4)} = -\Gamma\left[1 + \frac{\tanh\beta_\pm}{\beta_\pm^2}\frac{2\pi^2}{\sinh\left(\frac{\pi^2}{\beta_\pm}\right)}\right] - \tilde{\Omega}_\pm,$$

where the complex numbers $\Omega_\pm$ and $\tilde{\Omega}_\pm$ are given by

$$\Omega_\pm^2 = \Gamma^2 - 8\Delta\tanh\beta_\pm\cos(2\sigma_\pm)[\sinh\beta + \chi\partial_\beta Q_\beta(0)]_{\beta=\beta_\pm}, \tag{48}$$

$$\begin{aligned} \tilde{\Omega}_\pm^2 = {} & \Gamma^2\left[1 - \frac{\tanh\beta_\pm}{\beta_\pm^2}\frac{2\pi^2}{\sinh\left(\frac{\pi^2}{\beta_\pm}\right)}\right]^2 \\ & + 16\pi^4\chi\frac{\sinh^2\beta_\pm}{\beta_\pm^3\sinh\left(\frac{\pi^2}{\beta_\pm}\right)}\left[2(1-\chi)\frac{\sinh\beta_\pm}{\beta_\pm} + 2\chi\frac{\sinh^2\beta_\pm}{\beta_\pm^2\cosh\beta_\pm}\right. \\ & \left. - \Delta\frac{\tanh\beta_\pm}{\beta_\pm^3}\frac{\pi^2+4\beta_\pm^2}{6}\cos(2\sigma_\pm)\right]. \end{aligned} \tag{49}$$

The eigenvalues $\lambda_\pm^{(1)}$ and $\lambda_\pm^{(2)}$ describe the growth rates of the perturbations of the amplitude parameter β and phase parameter σ. The eigenvalues $\lambda_\pm^{(3)}$ and $\lambda_\pm^{(4)}$ describe the growth rates of the perturbations of the velocity parameter α and soliton center x.

The function $\beta\mapsto\sinh(\beta)+\chi\partial_\beta Q_\beta(0)$ is positive valued. Therefore, the real part of the eigenvalue $\lambda_-^{(1)}$ is positive and the stationary point labeled "–" is unstable. Besides, the real parts of the eigenvalues $\lambda_+^{(1)}$ and $\lambda_+^{(2)}$ are nonpositive for any

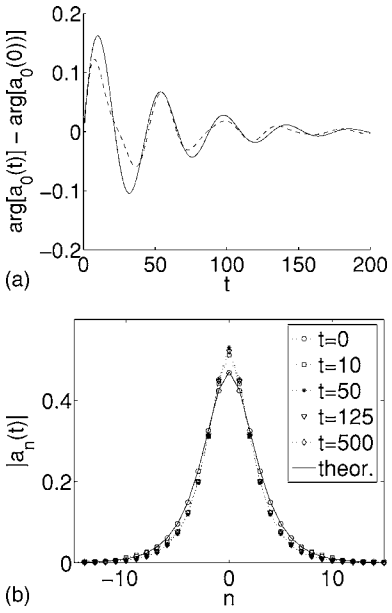

FIG. 10. Here $\chi=1$, $\omega=0.3$, $\delta=0.022$, $\gamma=0.02$. The T and t scales coincide. The initial condition is a soliton with $\sigma=\sigma_+$, $x_+=0$, $\alpha=0$, and $\beta=\beta_+-0.02=0.45$. The upper graph shows the argument of $a_0(t)$ (dashed line). The observed oscillations and damping are correctly predicted by the model. The period is $2\pi/\Omega_+=43.9$ and the exponential decay rate is $\Gamma=0.02$ (solid line). Note also, in the lower graph, that the stationary profile is not exactly the sech predicted by the AL theory, but a slightly deformed version.

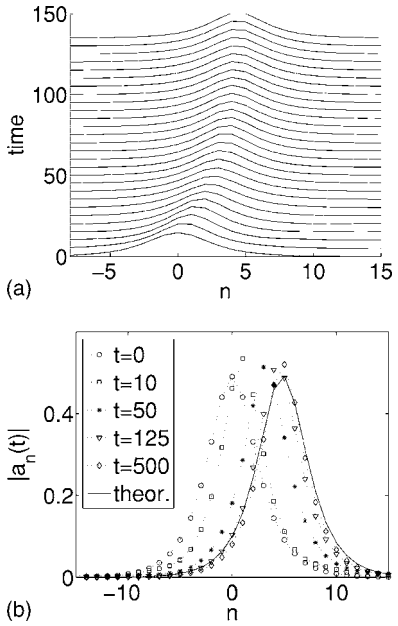

FIG. 11. Here $\chi=1$, $\omega=0.3$, $\delta=0.022$, $\gamma=0.02$. The initial condition is a soliton with $\sigma=\sigma_+$, $x_+=0$, $\alpha=0.1$, and $\beta=\beta_+=0.47$. We plot the soliton profiles $|a_n(t)|$ at different times, which exhibits the trapping of the moving soliton. The solid line is the theoretical stable stationary soliton centered at $x_F=4.82$ given by (50).

$\Gamma\geq 0$. The real parts of $\lambda_+^{(3)}$ and $\lambda_+^{(4)}$ are also nonpositive, which implies that the stationary point labeled "+" is stable.

When χ is large (say equal to 1), it is important to choose a suitable value ω so that the soliton parameter β_+ defined by Eq. (43) is small (more exactly, smaller than 0.5). Indeed, the theoretical analysis based on the perturbed IST is valid only in this case. Furthermore, numerical simulations show that Eq. (43) is not a stationary point for larger values of β_+, which shows the fundamental limitation in the perturbed IST. Within this region of parameters, the soliton parameters β and σ oscillate with the frequency Ω_+ given by Eq. (48) and they also experience an exponential decay with the rate Γ. The oscillation period and damping rate are confirmed by numerical simulations (Fig. 10).

Moreover, as in the AL case, the propagation of moving solitons is not supported, as the soliton velocity decays exponentially to 0. If we denote by α_0 the initial value of the parameter α, then the input soliton converges to its stationary form centered at

$$x_F=(1-\chi)[(\sinh\beta_+\sin\alpha_0)/(\beta_+\Gamma)] + \chi[(\sinh^2\beta_+\sin\alpha_0)/(\beta_+^2\cosh\beta_+\Gamma)]. \quad (50)$$

Notice that we have neglected higher-order term (in β) in this expression, which is consistent with the previous hypotheses and which gives a very accurate prediction for the final soliton position (see Fig. 11).

V. CONCLUSION

In this paper we have investigated the existence and stability properties of additional types of bright discrete solitons in discrete nonlinear Schrödinger-type models with damping and strong rapid drive. Stable stationary solitons are exhibited in the case of a general cubic nonlinearity. If the nonlinearity has the special AL form, then stationary solitons, moving solitons, and periodic trains of solitons are found to be stable solutions of the system. These results have been obtained by applying a perturbed inverse scattering transform to the averaged equation and confirmed by numerical simulations. This means that the inverse scattering theory is useful for probing the parameter space and exhibiting interesting phenomena. One of the problems that should be addressed for future consideration is the mechanisms responsible for the instabilities of the periodic cn and dn solutions for large drive, which seem to be different since a chaotic instability appears first in the dn case, while new patterns with different periods appear in the cn case.

ACKNOWLEDGMENT

F.Kh.A. is grateful to FAPESP for partial support.

[1] M. J. Ablowitz and Z. H. Musslimani, Phys. Rev. Lett. **87**, 254102 (2001).
[2] A. Trombettoni and A. Smerzi, Phys. Rev. Lett. **86**, 2353 (2001); F. Kh. Abdullaev, B. B. Baizakov, S. A. Darmanyan, V. V. Konotop, and M. Salerno, Phys. Rev. A **64**, 043606 (2001).
[3] F. Kh. Abdullaev, E. N. Tsoy, B. A. Malomed, and R. A. Kraenkel, Phys. Rev. A **68**, 053606 (2003).
[4] A. V. Ustinov, C. Coqui, A. Kemp, Y. Zolotaryuk, and M. Salerno, Phys. Rev. Lett. **93**, 087001 (2004).
[5] D. N. Christodoulides and N. Efremidis, Opt. Lett. **27**, 568 (2002).
[6] G. J. de Valcarcel and K. Staliunas, Phys. Rev. E **67**, 026604 (2003).
[7] U. Peschel, O. Egorov, and F. Lederer, Opt. Lett. **29**, 1909 (2004).
[8] A. V. Gorbach, S. Denisov, and S. Flach, Opt. Lett. **31**, 1702 (2006).
[9] M. Kollmann, H. W. Capel, and T. Bountis, Phys. Rev. E **60**, 1195 (1999).
[10] D. Hennig, Phys. Rev. E **59**, 1637 (1999).
[11] H. Susanto, Q. E. Hoq, and P. G. Kevrekidis, Phys. Rev. E **74**, 067601 (2006).
[12] I. V. Barashenkov, M. M. Bogdan, and V. I. Korobov, Europhys. Lett. **15**, 113 (1991).
[13] V. V. Alexeeva, I. V. Barashenkov, and D. E. Pelinovsky, Nonlinearity **12**, 103 (1999).
[14] M. Salerno, Phys. Rev. A **46**, 6856 (1992).
[15] N. K. Efremidis and D. N. Christodoulides, Phys. Rev. E **67**, 026606 (2003).
[16] A. A. Vakhnenko and Yu. B. Gaididei, Teor. Mat. Fiz. **68**, 350 (1986) [Theor. Math. Phys. **68**, 873 (1987)].
[17] D. Cai, A. R. Bishop, and N. Gronbech-Jensen, Phys. Rev. E **53**, 4131 (1996).
[18] E. V. Doktorov, N. P. Matsuka, and V. M. Rothos, Phys. Rev. E **68**, 066610 (2003).
[19] A. Khare and U. Sukhatme, J. Math. Phys. **43**, 3798 (2002); A. Khare, A. Lakshminarayan, and U. Sukhatme, *ibid.* **44**, 1822 (2003); Pramana, J. Phys. **62**, 1201 (2004).
[20] R. Scharf and A. R. Bishop, Phys. Rev. A **43**, 6535 (1991).
[21] A. Khare, K. Ø. Rasmussen, M. Salerno, M. R. Samuelsen, and A. Saxena, Phys. Rev. E **74**, 016607 (2006).
[22] O. O. Vakhnenko and V. O. Vakhnenko, Phys. Lett. A **196**, 307 (1995).